

## SENSOR SYNERGY OF ACTIVE AND PASSIVE MICROWAVE INSTRUMENTS FOR OBSERVATIONS OF MARINE SURFACE WINDS

N. Ebuchi

Institute of Low Temperature Science, Hokkaido University, N19-W8, Kita-ku, Sapporo 060-0819, Japan –  
ebuchi@lowtem.hokudai.ac.jp

**KEY WORDS:** Microwave Radiometer, Microwave Scatterometer, ADOES-II, GCOM-W, AMSR, SeaWinds, Marine Surface Wind

### ABSTRACT:

An example of sensor synergy of active and passive microwave instruments for observations of marine surface winds is demonstrated using data from the Advanced Earth Observing Satellite-II (ADEOS-II), which carried a Ku-band microwave scatterometer, SeaWinds, and the Advanced Microwave Scanning Radiometer (AMSR). Scalar wind speed observed by AMSR was evaluated by using wind speed observed by SeaWinds. The intercomparison between the AMSR and SeaWinds wind speeds was largely contributed to improvements of the wind retrieval algorithm for AMSR. The latest version of AMSR wind speed agrees well with buoy and SeaWinds data with negligibly small bias and root-mean-squared difference of approximately  $1.5 \text{ ms}^{-1}$ . A discontinuous trend in the wind speed, which was discernible in the earlier versions, was much reduced in the latest version. Wind speed bias which depends on the relative wind direction was significantly reduced compared to the previous versions. Rain flag algorithm developed for the SeaWinds wind products was also assessed using rain data derived from AMSR. Global statistical analyses indicated significant improvements of the rain flag algorithm compared to the previous version. Evaluation of wind speed algorithm of AMSR and rain flag algorithm for SeaWinds will contribute not only to improvements of the wind products of AMSR and SeaWinds on ADEOS-II but also to those of AMSR-E on Aqua and SeaWinds on QuikSCAT, which are not accompanied by active and passive microwave sensor, respectively.

### 1. INTRODUCTION

The Advanced Earth Observing Satellite-II (ADEOS-II) was launched by the National Space Development Agency of Japan (NASDA) on 14 December 2002. The mission carried five sensors including the SeaWinds and the Advanced Microwave Scanning Radiometer (AMSR), which measure near-surface winds over the global oceans under all weather and cloud conditions. SeaWinds is a microwave scatterometer that measures wind speed and directions over the ocean surface. AMSR is a multi-frequency, dual-polarized microwave radiometer that measures microwave emissions from the Earth's surface and atmosphere. AMSR measures scalar wind speed over the oceans together with various physical parameters of the ocean surface and atmosphere including sea surface temperature, integrated water vapor, liquid water content, and precipitation. Simultaneous observations of the marine surface winds by the active and passive microwave sensors on the same satellite presented a unique opportunity to assess the synergy of active and passive microwave sensors. Wind retrieval algorithms for the scatterometer and microwave radiometer can be improved by wind data intercomparisons.

In this paper, scalar wind speeds observed by AMSR are evaluated by using wind speeds observed by SeaWinds together with data from ocean buoys. Rain flag algorithm developed for the SeaWinds wind products was also assessed using rain data derived from AMSR.

Evaluation of wind speed algorithm of AMSR and rain flag algorithm for SeaWinds will contribute not only to improvements of the wind products of AMSR and SeaWinds on ADEOS-II but also to those of AMSR-E on Aqua and SeaWinds on QuikSCAT, which are not accompanied by active and passive microwave sensor, respectively.

### 2. DATA

#### 2.1 AMSR

The AMSR level-2 standard product/sea surface wind, which was processed and distributed by the Japan Aerospace Exploration Agency (JAXA), was utilized in this study. The AMSR standard algorithm developed by Shibata (2002) was used to derive wind speed from brightness temperatures. The first version (version 1) was released to users in December 2003. Based on evaluations of the data product, the wind retrieval algorithm was refined and the entire data product was reprocessed using the new algorithm (version 5). The wind data of versions 1 to 5 spanning 10 April 2003 to 24 October 2003 are analyzed in this paper. Evaluations of the previous versions of the AMSR wind data (versions 3 and 4) were presented by Ebuchi (2006, 2009).

#### 2.2 SeaWinds

The SeaWinds science data product, level 2B, which was processed and distributed by the National Aeronautics and Space Administration (NASA)/Jet Propulsion Laboratory (JPL) Physical Oceanography Distributed Active Archive Center (PO.DAAC), are utilized in this study. The wind data were produced using a maximum-likelihood estimator (MLE) with the QSCAT-1 geophysical model function and a median filter ambiguity removal algorithm with the numerical weather product (NWP) initialization. The spatial resolution of the wind data is 25 km and the reference level of the wind vectors is 10 m. The impact-based multidimensional histogram (IMUDH) rain flag was applied to indicate the presence of rain. Data observed from 10 April 2003 to 24 October 2003 were used in the present study.

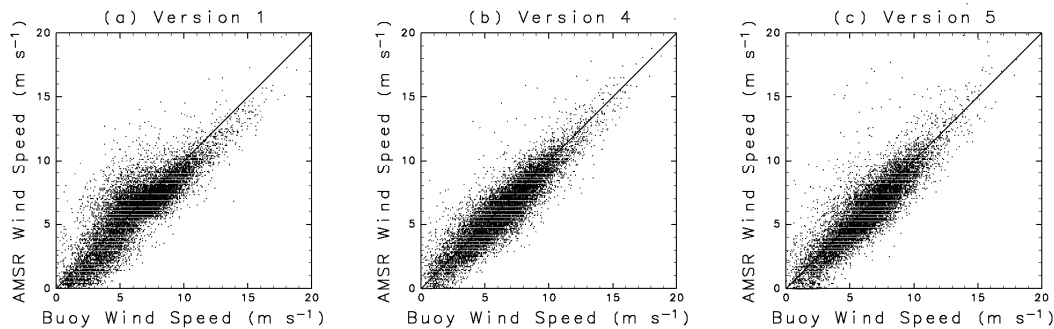


Figure 1. Comparison of wind speeds observed by AMSR with buoy data. Versions (a) 1, (b) 4, and (c) 5.

Version	1	4	5
Number of data	11865	11142	10655
Bias ( $\text{m s}^{-1}$ )	-0.22	-0.24	-0.31
Rms difference ( $\text{m s}^{-1}$ )	1.41	1.17	1.29
Correlation coefficient	0.855	0.902	0.883

Table 1. Statistics describing wind speeds observed by AMSR and buoy data.

### 2.3 Ocean Buoys

We collected data from offshore buoys operated by the National Data Buoy Center (NDBC), the Tropical Atmosphere Ocean/Triangle Trans-Ocean Buoy Network (TAO/TRITON) and the Pilot Research Moored Array in the Tropical Atlantic (PIRATA) to compare them with the AMSR wind data. Data from 34 NDBC, 48 TAO/TRITON, and 7 PIRATA buoys were utilized. Only those buoys located offshore and in deep water were selected. Details of the NDBC and TAO buoys, instruments, and stations were described by Meindl and Hamilton (1992) and McPhaden (1995), respectively. The PIRATA buoys are identical to the TAO buoys. Data with a high sampling interval of 10 min. were utilized. The wind speed measured by the buoys at various heights above the sea surface was converted to equivalent neutral wind speed at a 10-m height using the method proposed by Liu and Tang (1996).

## 3. EVALUATION OF AMSR WIND SPEED

### 3.1 Comparison of Wind Speed Observed by AMSR with Buoy Data

The AMSR wind data and buoy observations were collocated in time and space. AMSR wind observation cells closest in space to the buoy locations and the buoy data closest in time to the AMSR observations were chosen. The temporal differences and spatial separations between the AMSR and buoy observations were restricted to less than 10 min. and 10 km, respectively.

Figure 1 compares the three versions of AMSR wind speed with buoy observations. Statistical values of the comparisons are listed in Table 1. It is clear that version 1 winds exhibit a

discontinuous trend around  $5\text{--}6 \text{ m s}^{-1}$ , as reported by previous studies (Ebuchi, 2006, 2009). In wind speeds lower than  $5 \text{ m s}^{-1}$ , the wind speeds of the version 1 are systematically lower than those from the buoys. These systematic trends have been considerably reduced in the versions 4 and 5. The  $-0.31 \text{ m s}^{-1}$  bias (AMSR-buoy) and rms difference of  $1.29 \text{ m s}^{-1}$  are comparable to or slightly larger than the results of wind speed comparisons observed by QuikSCAT/SeaWinds (Ebuchi et al. 2002) and ADEOS-II/SeaWinds (Ebuchi, 2006) with buoy data.

### 3.2 Intercomparison of Wind Speed Observed by AMSR and SeaWinds

Wind data observed globally by SeaWinds and AMSR along identical satellite orbits were collocated by wind cell to cell. All the flagged data, including rain-flagged data, were discarded. Only data observed between latitudes  $65^{\circ}\text{S}$  and  $65^{\circ}\text{N}$  were used to avoid contamination by sea ice. The number of collocated data points is greater than 60 million. Figure 2 compares wind speeds observed by AMSR and SeaWinds for the three versions of the AMSR data. The density of data points in  $0.1 \times 0.1 \text{ m s}^{-1}$  bins is shown by the shading. Statistics describing the comparisons are listed in Table 2.

Figure 2 more clearly exhibits the systematic trends in the version 1 wind product that appear in the buoy comparison (Fig. 1). The large number of AMSR-SeaWinds collocated data clearly demonstrates that the discontinuous wind speed trends of version 1 have been eliminated in versions 4 and 5 through algorithm improvement. For version 5, the bias (AMSR-SeaWinds) and rms difference are  $-0.13 \text{ m s}^{-1}$  and  $1.24 \text{ m s}^{-1}$ , respectively, indicating that the wind speeds observed by the two sensors are in good agreement.

Version	1	4	5
Number of data	67048608	63071149	62218021
Bias ( $\text{m s}^{-1}$ )	-0.10	-0.08	-0.13
Rms difference ( $\text{m s}^{-1}$ )	1.54	1.16	1.24
Correlation coefficient	0.940	0.952	0.948

Table 2. Statistics describing wind speeds observed by AMSR and SeaWinds.

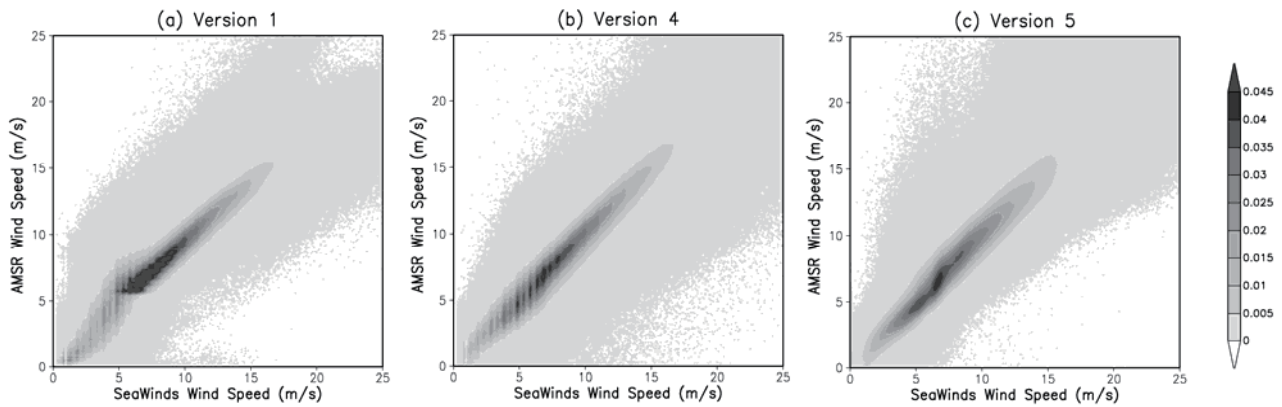


Figure 2. Comparison of wind speeds observed by AMSR and SeaWinds. Versions (a) 1, (b) 4, and (c) 5.

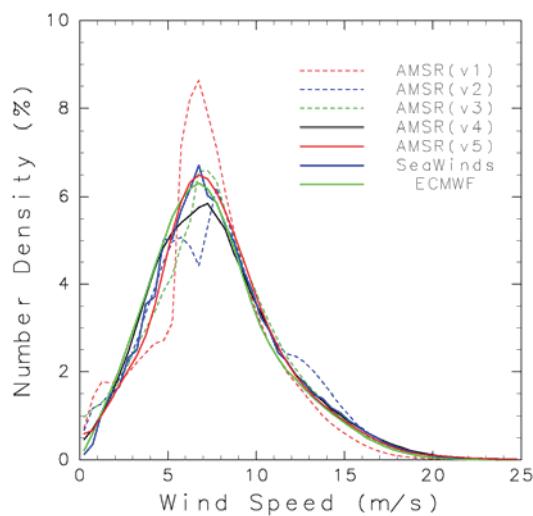


Figure 3. Comparison of global wind speed histograms.

### 3.3 Comparison of Global Wind Speed Histograms

Histograms of wind speed over the global oceans were calculated from all the wind speed data from latitudes 65°S to 65°N and for 7 months from April to October 2003. Comparison of global wind speed histograms calculated from the three AMSR wind product versions and SeaWinds wind speeds is shown in Fig. 3. For reference, a histogram calculated from the European Centre for Medium-range Weather Forecasts (ECMWF) analysis (2.5° x 2.5°, 12-hour intervals) in the same period is also shown in the figure.

The histograms of SeaWinds and ECMWF wind speeds are in good agreement. Version 1 of the AMSR wind product exhibits significant deviation from those of the SeaWinds and ECMWF winds, reflecting the discontinuities shown in Figs. 1(a) and 2(a). The histogram of version 4 AMSR winds has a lower number density at the peak wind speed. The histograms of version 5 AMSR winds are closer to those of SeaWinds and ECMWF winds than histograms of earlier versions over the whole wind speed range. The evolution of the global wind speed histograms clearly demonstrates improvements in the AMSR wind retrieval algorithm from the earlier versions to the latest version.

### 3.4 Wind Speed Bias Depending on Relative Wind Direction

Figure 4 shows the wind speed bias (AMSR-SeaWinds) as a function of the SeaWinds wind speed and wind direction relative to the AMSR-looking direction. In AMSR versions 3 and 4, wind speed bias depending on the relative wind direction is discernible with a magnitude greater than 1.5 m/s. The relative modulation of the bias depending on the wind direction is reduced to around 1 m s<sup>-1</sup> or less by the algorithm improvement to the version 5.

Figure 5 compares the bias at wind speed of 10 ms<sup>-1</sup>. It is clearly shown that the amplitude of bias modulation is reduced 1.2 m s<sup>-1</sup> (versions 3 and 4) to 0.8 m s<sup>-1</sup> (version 5).

## 4. ASSESSMENT OF SEAWINDS RAIN FLAG

Scatterometers measure the normalized radar cross section (sigma-0) of the ocean surface. Such measurements are then used to infer the speed and direction of ocean surface winds. When rain is present, measurements of the ocean surface sigma-0 become contaminated for several reasons. Some of the transmitted energy is scattered back towards the scatterometer by rain drops and never reaches the ocean surface. Energy backscattered from the rain can constitute a significant but unknown portion of the measured echo energy. Some of the transmitted energy is scattered and/or absorbed by the rain and is never measured by the scatterometer. This has the effect of attenuating the echo energy from the ocean. Additionally, the rain may affect roughness of the ocean surface and change its radar cross section.

In the QuikSCAT/SeaWinds and ADEOS-II/SeaWinds missions, the Multidimensional Histogram (MUDH) Rain Flag and Impact-based Multidimensional Histogram (IMUDH) Rain Flag algorithms were designed to indicate the presence of rain on a wind vector cell by wind vector cell basis. Performance of these algorithms was assessed using precipitation data observed by AMSR. Collocated data set was produced by using global wind measurements by SeaWinds and precipitation measurements by AMSR in the same orbit for a period of 6 months from April to October 2003. Over 52 million collocated data points were obtained.

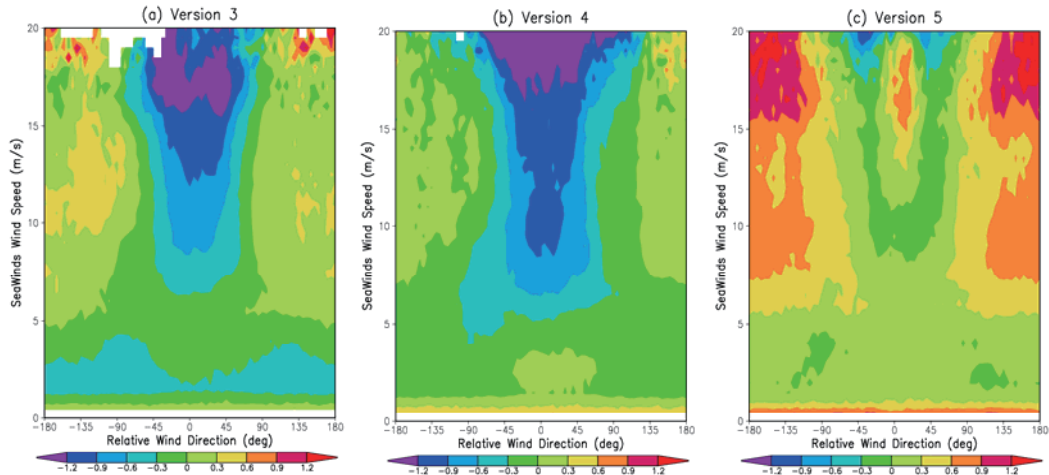


Figure 4. Wind speed bias (AMSR-SeaWinds) in  $m s^{-1}$  as a function of relative wind direction and SeaWinds wind speed. Versions (a) 3, (b) 4, and (c) 5.

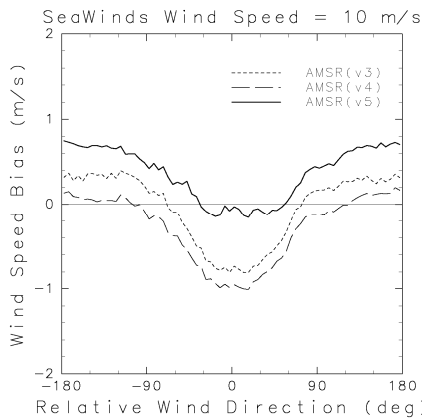


Figure 5. Wind speed bias (AMSR-SeaWinds) at SeaWinds wind speed of  $10 m s^{-1}$ .

and over the entire mission period of 7 months decreased from 7.2% (MUDH) to 5.8% (IMUDH). Except for outer cells, the rain flag rate does not largely depend on the cross-track cell location.

False rain flag rate was estimated by calculating the rate of rain-flagged cell under conditions of AMSR rain rate less than  $0.1 mm h^{-1}$ . In Fig. 7, the false rain rate is shown as functions of (a) the cross-track cell location and (b) wind speed. It is clearly shown that the false rate has been significantly reduced from MUDH to IMUDH. Dependence on the cross-track cell location is also smaller for IMUDH. Although the MUDH algorithm exhibits over-flagging at high wind speed ranges, the over-flagging trend has been significantly improved in the wind products reprocessed by the IMUDH algorithm. These results demonstrate the significant improvements of the rain flagging algorithm from MUDH to IMUDH.

5. CONCLUSION

In this paper, an example of sensor synergy of active and passive microwave instruments for observations of marine surface winds is demonstrated using the data from ADEOS-II, which carried a Ku-band microwave scatterometer, SeaWinds, and the Advanced Microwave Scanning Radiometer (AMSR).

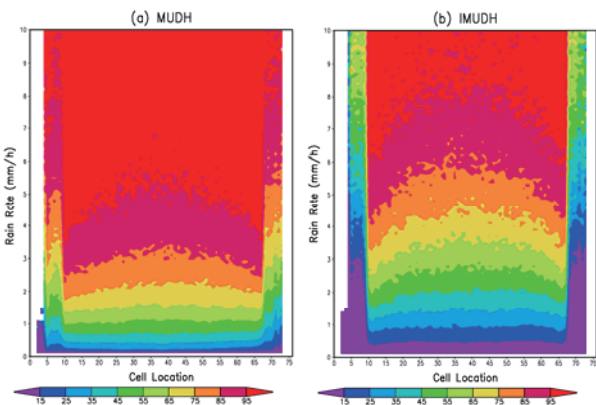


Figure 6. Rate of rain flagged data as a function of cross-track cell location and AMSR rain rate. (a) MUDH, and (b) IMUDH

Figure 6 shows the rate of flagged data as a function of the AMSR rain rate and cross-track wind vector cell location of the SeaWinds, where 1 and 76 indicate outer wind vector cells and 37 and 38 are the inner cells. It is shown that the previous version (MUDH) flags more than the recent version (IMUDH) in general. Overall rain flag rate averaged over the global ocean

Marine surface winds observed by AMSR were evaluated by comparison with offshore moored buoy observations and wind speed data observed by SeaWinds on the same satellite. Wind speeds measured by the latest AMSR wind product (version 5) exhibited good agreement with buoy data in general, with an rms difference of  $1.3 m s^{-1}$ . A systematic bias observed in earlier versions has been eliminated by algorithm refinements. Intercomparison of wind speeds observed globally by SeaWinds and AMSR on the same orbits also showed good agreement. Global wind speed histograms of the SeaWinds data and ECMWF analyses agreed precisely with each other. The latest AMSR wind product (version 5) also agrees more closely with SeaWinds data and ECMWF analyses than earlier versions over the whole wind speed range. Wind speed bias which depends on the relative wind direction was significantly reduced compared to the previous versions. The present study demonstrated the efficiency of using active and passive microwave sensors in conjunction to improve wind retrieval algorithms.

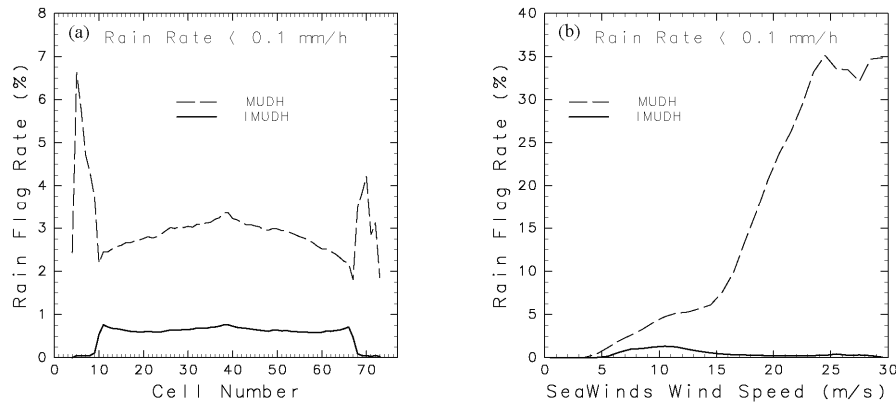


Figure 7. False rain flag rate as functions of (a) the cross-track cell location and (b) wind speed.

Rain flag algorithm developed for the SeaWinds wind products was also assessed using rain data derived from AMSR. Global statistical analyses indicated significant improvement of the rain flag algorithm (IMUDH) compared to the previous versions (MUDH).

These results clearly exhibited importance of the sensor synergy of the active and passive microwave sensors, and demonstrated needs of future missions (e.g., GCOM-W series) with a combination of microwave scatterometer and radiometer onboard the same satellite to achieve simultaneous observation.

#### ACKNOWLEDGMENT

The author gratefully acknowledges funding support from the Japan Aerospace Exploration Agency (JAXA), in addition to the assistance of Dr. Akira Shibata, Meteorological Research Institute, Japan Meteorological Agency, for helpful discussion and information concerning the AMSR wind retrieval algorithms and data processing. The National Data Buoy Center (NDBC) and the Tropical Ocean Atmosphere (TAO) Project Office provided the buoy data. The SeaWinds and AMSR data products used in this study were obtained from the NASA/JPL PO-DAAC and JAXA, respectively. The author expresses his sincere thanks to these data providers.

#### REFERENCES

- Ebuchi, N., 2006, Evaluation of marine surface winds observed by SeaWinds and AMSR on ADEOS-II. *J. Oceanogr.*, 62, pp. 293-301.
- Ebuchi, N., 2009, Evaluation of wind speed observed by AMSR using data from ocean buoys and SeaWinds. *J. Remote Sens. Soc. Jpn*, 29, pp.174-178.
- Ebuchi, N., H. C. Graber, and M. J. Caruso, 2002, Evaluation of wind vectors observed by QuikSCAT/SeaWinds using ocean buoy data. *J. Atmos. Oceanic Tech.*, 19, pp. 2049-2062.
- Meindl, E. A., and G. D. Hamilton, 1992, Programs of the National Data Buoy Center. *Bull. Amer. Meteorol. Soc.*, 73, pp. 985-993.
- McPhaden, M. J., 1995, The Tropical Atmosphere Ocean array is completed. *Bull. Amer. Meteorol. Soc.*, 76, pp. 739-741.
- Liu, W. T., and W. Q. Tang, 1996, Equivalent neutral wind. JPL Publ. 96-19, Jet Propul. Lab., Pasadena, Calif., U.S.A., pp. 8.
- Shibata, A., 2002, AMSR/AMSR-E sea surface wind speed algorithm. *EORC Bull.*, 9, JAXA, Tokyo, Japan, pp. 94.